HHS Public Access

Author manuscript

Exp Eye Res. Author manuscript; available in PMC 2023 December 01.

Published in final edited form as:

Exp Eye Res. 2022 December ; 225: 109265. doi:10.1016/j.exer.2022.109265.

CXCR3 deletion aggravates corneal neovascularization in a corneal alkali-burn model

Shengguo Li[a,1], **Shuizhen Shi**[a], **Fan Xia**[a], **Ban Luo**[a], **Yonju Ha**[a], **Jonathan Luisi**[a,b], **Praveena K. Gupta**[a], **Kevin H. Merkley**[a], **Massoud Motamedi**[a], **Hua Liu**[a,**], **Wenbo Zhang**[a,c,*]

[a]Department of Ophthalmology & Visual Sciences, University of Texas Medical Branch, Galveston, TX, USA

[b]Department of Pharmacology and Toxicology, University of Texas Medical Branch, Galveston, TX, USA

[c]Departments of Neuroscience, Cell Biology & Anatomy, University of Texas Medical Branch, Galveston, TX, USA

Abstract

Corneal neovascularization can cause devastating consequences including vision impairment and even blindness. Corneal inflammation is a crucial factor for the induction of corneal neovascularization. Current anti-inflammatory approaches are of limited value with poor therapeutic effects. Therefore, there is an urgent need to develop new therapies that specifically modulate inflammatory pathways and inhibit neovascularization in the cornea. The interaction of chemokines and their receptors plays a key role in regulating leukocyte migration during inflammatory response. CXCR3 is essential for mediating the recruitment of activated T cells and microglia/macrophages, but the role of CXCR3 in the initiation and promotion of corneal neovascularization remains unclear. Here, we showed that the expression of CXCL10 and CXCR3 was significantly increased in the cornea after alkali bum. Compared with WT mice, $CXCR3^{-/-}$ mice exhibited significantly increased corneal hemangiogenesis and lymphangiogenesis after alkali burn. In addition, exaggerated leukocyte infiltration and leukostasis, and elevated expression of inflammatory cytokines and angiogenic factor were also found in the corneas of $CXCR3^{-/-}$ mice subjected to alkali burn. With bone marrow (BM) transplantation, we further demonstrated that the deletion of CXCR3 in BM-derived leukocytes plays a key role in the acceleration of alkali burn–induced corneal neovascularization. Taken together, our results suggest that upregulation of CXCR3 does not exhibit its conventional action as a proinflammatory cytokine but instead serves as a self-protective mechanism for the modulation of inflammation and maintenance of corneal avascularity after corneal alkali burn.

*Corresponding author. Ophthalmology & Visual Sciences, University of Texas Medical Branch, 301 University Boulevard, Galveston, TX, 77555-0144, USA. we2zhang@utmb.edu (W. Zhang). **Corresponding author. Ophthalmology & Visual Sciences, University of Texas Medical Branch, 301 University Boulevard, Galveston, TX, 77555-0144, USA. hualiu@utmb.edu (H. Liu).

[1]Present address: Department of Ophthalmology, Changsha Aier Eye Hospital, Changsha, 410011, Hunan Province, China.

Declaration of competing interest

None.

Appendix A. Supplementary data

Supplementary data to this article can be found online at https://doi.org/10.1016/j.exer.2022.109265.

Keywords

Corneal neovascularization; Inflammation; Alkali burn; CXCR3

1. Introduction

The cornea's avascular and transparent properties are required to sustain visual acuity under normal conditions. Acute ocular chemical (alkalis and acids) burns can cause severe complications and profound vision loss (Eslani et al., 2014). Due to the lipophilicity of alkalis, they can more readily penetrate the cornea leading to more severe damage than acids. Corneal neovascularization is a serious complication (Anderson et al., 2014) after exposure to alkali, and can result in persistent corneal inflammation, clouding and scarring that diminish the success of subsequent penetrating keratoplasty (Nicholas and Mysore, 2021). Conventional medical approaches including amniotic membrane transplantation (Kobayashi et al., 2003), photodynamic therapy (Wang et al., 2012) and fine needle diathermy (Spiteri et al., 2015) have all been used to restrain corneal neovascularization. These treatments, nevertheless, have limited value and poor therapeutic effects (Vivanco-Rojas et al., 2020).

Unbalanced proangiogenic and antiangiogenic factors are well-known mechanisms of corneal neovascularization (Sharif and Sharif, 2019). Multiple cell types in the cornea, including immune cells, corneal epithelial and endothelial cells and stromal keratocytes, can release proangiogenic factors, such as vascular endothelial growth factor (VEGF), as a result of persistent ocular inflammatory condition (Nicholas and Mysore, 2021; Philipp et al., 2000). Hence, inflammation is a crucial factor contributing to the induction of corneal neovascularization. Topical corticosteroids can reduce inflammatory cell infiltration and stabilize lysosomal membranes (Kim et al., 2021; Leibowitz, 1980), but only can be used for the first week after alkali burn. Prolonged use of corticosteroids increases the risk of corneal melting, reinfection, glaucoma, and cataract formation (Donshik et al., 1978). Currently, the treatment with anti-VEGF antibodies to prevent corneal neovascularization seems to have a promising future for the management of alkali burn (Giannaccare et al., 2020), but it is important to recognize that topical anti-VEGF treatments only work by shrinking newly formed blood vessels but fail to alter the fundamental pathology (Keating and Jacobs, 2011). Anti-VEGF agents also require treatments over a sustained period of time and may cause delayed wound healing accompanied by the progression of stromal thinning in the cornea (Kim et al., 2009; Koenig et al., 2009). Therefore, it is essential to further investigate the mechanisms of corneal neovascularization with the goal of discovering additional molecules/pathways that can be targeted enabling more effective regulation of inflammatory cell recruitment and activation during the process of corneal neovascularization.

CXCR3 is a G protein-coupled chemokine receptor of the CXC chemokine receptor family that binds CXCL9, CXCL10, and CXCL11 chemokines (Clark-Lewis et al., 2003). CXCR3 is required for the recruitment of activated microglia/macrophages and T cells (de Jong et al., 2008; Torraca et al., 2015). In $CXCR3^{-/-}$ mice, skin wound repair showed delayed healing, continual inflammation, and persistent angiogenesis (Yates et al., 2009). It has been

shown that stimulation of the CXCL10/CXCR3 signaling increases microglial recruitment and triggers neuronal cell death in a variety of neurodegenerative studies (Ha et al., 2015; Rappert et al., 2004). However, the role of the CXCR3 pathway in the process of corneal inflammation and neovascularization is not yet fully understood.

In the present study, we showed that CXCR3 signaling was activated in a mouse model of alkali burn, and CXCR3 deficiency exaggerates ocular inflammation, resulting in increased corneal hemangiogenesis and lymphangiogenesis.

2. Material and methods

2.1. Animals

C57BL/6 wild type (WT) (#000664) and CXCR3$^{-/-}$ (#005796) mice were originally purchased from the Jackson laboratory and have been bred in the animal facility of the University of Texas Medical Branch (UTMB). The genotype of CXCR3$^{-/-}$ breeders was confirmed by genotyping using DNA from tails according to the protocol provided by the Jackson Laboratory as describe in our previous publication (Ha et al., 2017). Male WT and CXCR3$^{-/-}$ mice (8–10 weeks old) were used. Animal research followed the National Institutes of Health guide for the care and use of Laboratory animals and adhered to the Association for Research in Vision and Ophthalmology Statement for the Use of Animals in Ophthalmic and Vision Research, and was approved by the UTMB's Institutional Animal Care and Use Committee.

2.2. Alkali burn model

A mixture of ketamine (100 mg/kg) and xylazine (10 mg/kg) was injected (i.p.) to anesthetize mice. Under a surgical microscope, a piece of round filter paper with a diameter of 2 mm which was soaked in 3 μL of 1M NaOH was placed on the central cornea of the right eyes for 30 s with sterile forceps to cause an acute alkali burn. After removing the filter paper, the eye was gently rinsed twice with 10 mL 1x PBS using a 10 mL syringe to eliminate any residual NaOH. The development of corneal opacity and neovascularization was photographed at 0, 3, 7, and 14 days after alkali burn (Luisi et al., 2021; Tarff et al., 2022). The degree of corneal neovascularization and corneal opacity were evaluated using a published grading system (Anderson et al., 2014).

2.3. Optical Coherence Tomography

After mice were anesthetized, one drop of Genteal tears (Alcon Laboratories, Fort Worth, TX) was applied to the eye to maintain corneal hydration. A spectral-domain OCT system (Envisu R2200; Bioptigen, Durham, NC) was used to image the anterior segment of the eye at 0, 3, 7 and 14 days after alkali burn. Full corneal thickness was measured from epithelium to endothelium using ImageJ (Li et al., 2022; Luisi et al., 2021). Based on the separation distance between corneal endothelium border and the root of the iris seen in OCT images, we scored changes in anterior chamber angle using the Shaffer grading system (Lange et al., 2009).

2.4. Immunostaining for corneal cryosections

At 3 days after alkali burns, eyeballs were collected for cryosections. Immunostaining was carried out as previously described (Xia et al., 2021). The following antibodies were applied: CXCR3 (1:400, BD Pharmingen, San Diego, CA), VEGF (1:500, Abcam, Cambridge, MA), CD45 (1:400, BD Bioscience, San Jose, CA), and MPO (1:400, Thermo Fisher Scientific, Waltham, MA). Alexa Fluor 488- or 594-conjugated secondary antibodies were applied (1:1,000, Life Technologies, Waltham, MA) at room temperature for 1 h. Finally, sections were mounted with medium containing DAPI (Abcam) and images were taken by confocal microscope (Carl Zeiss Inc, Thornwood, NY).

2.5. Leukostasis and immunostaining in corneal flatmounts

Leukostasis was performed as previously reported (Liu et al., 2020). Briefly, mice were anesthetized deeply at 14 days after alkali burn. After cardiac lavage was performed to remove non-adherent blood cells, 10 mL rhodamine-coupled Concanavalin A (Con A) (40 μg/mL in PBS [pH 7.4]; Vector Laboratories, Burlingame, CA) was perfused to label adherent leukocytes and blood vessels.

After perfusion was completed, the eyeballs were collected and preserved in 4% paraformaldehyde (PFA) for 1 h. Corneas were dissected from the eyeballs and radially cut into four petals. The corneas were washed with PBS and blocked with a mixture of 5% normal donkey serum and 0.5% Triton-X-100 for 2 h. Next, the corneas were incubated with antibodies against CD31 (1:400, 553,369, BD Biosciences) and LYVE-1 (1:400, AF2125, R&D System, Minneapolis, MN) to identify new blood vessels and lymphatic vessels at 4 °C overnight. Subsequently, the corneas were incubated with secondary antibodies (1:400, Life Technologies) – Alexa Fluor 674 for CD31 (purple) or Alexa Fluor 488 for LYVE-1 (green) at 4 °C for 4 h. Lastly, the corneas were mounted in preparation for confocal microscopy allowing for capturing four non-overlapping images at the periphery of each corneal flatmount. The areas of corneal hemangiogenesis and lymphangiogenesis were measured by ImageJ. Adherent leukocytes labeled by Con A were then counted under the microscope.

2.6. Bone marrow (BM) transplantation

Recipient WT or CXCR3$^{-/-}$ mice at 6 weeks of age were pre-conditioned by irradiation (Liu et al., 2020). Mice's heads and eyes were protected by a lead shield. Extracted bone marrow cells were derived from the femur and tibia of donor mice. Following washing, bone marrow cells were resuspended in PBS without Ca^{2+}/Mg^{2+} before injection. Cell suspension of 200 μL with 2.0×10^7 cells was injected into the tail vein of recipient mice within 24 h after irradiation. Lastly, chimeric mice were subjected to alkali burn 6 weeks after bone marrow transplantation.

2.7. Quantitative real-time polymerase chain reaction (qRT-PCR)

At 3 days after alkali burns, the corneas were collected, homogenized and lysed for qRT-PCR as described previously (Li et al., 2021). The sequences of PCR primers used in our study are listed in Table 1.

2.8. Statistics

Statistical analyses were achieved using GraphPad Prism software (GraphPad Software Inc., La Jolla, CA) as described (Liu et al., 2020). All data were shown as mean ± SEM. A $p < 0.05$ was considered statistically significant.

3. Results

3.1. CXCL10 and CXCR3 are upregulated in the cornea after alkali burn

To investigate whether CXCR3 signaling is involved in corneal neovascularization after alkali burn, we initially inspected the expression of ligand CXCL10 and its receptor CXCR3 in the cornea at 3 days after alkali burn using quantitative PCR and immunostaining. The RNA level of CXCL10 was significantly elevated in the cornea of WT mice after alkali burn ($n = 4–5$, $*p < 0.05$) (Fig. 1A). The immunoreactivity of CXCR3 was mainly localized in the cells of the epithelial layer in control cornea. However, after alkali burn, its immunoreactivity was significantly increased in cells in both epithelial and stromal layers, including $CD45^+$ leukocytes (Fig. 1B and C, Supplementary Fig. 1) ($n = 5$, $***p < 0.001$). No specific CXCR3 immunoreactivity was observed in $CXCR3^{-/-}$ groups (Fig. 1B, lower panels), implicating the specificity of anti-CXCR3 staining. These data demonstrate that in response to alkali burn, both CXCL10 and CXCR3 levels are elevated in the cornea, suggesting that the CXCR3 signaling is potentially involved in corneal pathology after alkali burn.

3.2. Deficiency of CXCR3 aggravates corneal neovascularization after alkali burn

To identify the role of CXCR3 signaling in corneal neovascularization, both WT and $CXCR3^{-/-}$ mice were subjected to alkali burns. Bright-field images were taken under microscopy before alkali burn and at different time points after injury (0, 3, 7 and 14 days). Clinical scoring system was applied to assess corneal opacity and neovessel formation in the cornea as previously described (Anderson et al., 2014). As shown in Fig. 1D, alkali burn caused corneal opacity and corneal neovascularization in both WT and $CXCR3^{-/-}$ mice. Corneal opacity progressively increased after alkali burn, but there were no differences between WT and $CXCR3^{-/-}$ groups (Fig. 1D and E) ($n = 6$). Corneal neovascularization in WT group peaked on the 7th day post treatment and then decreased, whereas corneal neovascularization in $CXCR3^{-/-}$ group continued to expand after alkali burn. As a result, the degree of corneal neovascularization in $CXCR3^{-/-}$ group was significantly higher than that in WT group at 14 days after alkali burn (Fig. 1D and F) ($n = 6$, $****p < 0.0001$).

To further analyze and compare the extent of corneal neovascularization in WT to $CXCR3^{-/-}$ mice after alkali burn, corneal hemangiogenesis and lymphangiogenesis were examined by immunostaining with endothelial cell marker (CD31, purple) and lymphatic vessel marker (LYVE-1, green) at 14 days after alkali burn. In untreated corneas, there were no obvious differences in limbal vessels and lymphatic vessels between WT and $CXCR3^{-/-}$ groups (Fig. 2A). However, hemangiogenesis and lymphangiogenesis were significantly increased in $CXCR3^{-/-}$ corneas compared with WT corneas at 14 days after alkali burn (Fig. 2B-D) ($n = 5$, $**p < 0.01$).

3.3. CXCR3 deletion does not affect corneal thickness and the closure of anterior chamber angle after alkali burn

Beyond seriously damaging to the cornea, alkali burn can lead to the closure of the anterior chamber angle. To analyze temporal changes in the architecture of the anterior segment of the eye after alkali burn, non-invasive Optical Coherence Tomography (OCT) was used to visualize the structures of cornea and anterior chamber angle. Although corneal thickness was increased after alkali burn, no distinguishable differences were observed between WT and CXCR3$^{-/-}$ mice at various time points (Fig. 3A and C), suggesting that there was no apparent correlation between corneal thickness and the degree of corneal neovascularization.

The anterior chamber angle closed over time after alkali burn, which was induced by the complete adhesion of iris root to corneal endothelium border, with no void space between them (Fig. 3B). Analysis of the score assigned to the degree of the anterior chamber angle closure at various time points post treatment using the Shaffer grading system did not show any differences between WT and CXCR3$^{-/-}$ mice (Fig. 3D).

3.4. Deficiency of CXCR3 increases inflammatory response

Since inflammation plays a key role in neovascularization, we evaluated corneal inflammation by histopathology. Leukocytes were stained with CD45 antibody and neutrophils were stained with MPO antibody at 3 days after alkali burn, respectively (Fig. 4A). We found that the number of CD45^{+} leukocytes and MPO^{+} neutrophils was dramatically increased in the corneas of CXCR3$^{-/-}$ mice after alkali burn compared with WT mice (Fig. 4A, C, 4D) (n = 4–5, ****p < 0.0001). To further evaluate the effect of CXCR3 signaling on promoting inflammation after alkali burn, leukostasis was performed and adherent leukocytes to the corneal vasculature were quantified following Con A perfusion in both WT and CXCR3$^{-/-}$ mice. While fewer adherent leukocytes were found in corneal vasculature in WT and CXCR3$^{-/-}$ control mice, the number of adherent leukocytes in corneal vasculature was dramatically increased after alkali burn, which was significantly exaggerated by CXCR3 deletion (Fig. 4B and E) (n = 4, *p < 0.05, **p < 0.01). Furthermore, consistent with the observed differences in histopathological findings, real-time RT-PCR analysis revealed that the mRNA expression of proinflammatory/angiogenic genes including IL-1β, IL-6, iNOS, CCL2, VEGF and PAI-1 was significantly elevated in the cornea at 3 days after alkali burn (Fig. 5), and CXCR3 deficiency led to further increases in the expression of IL-1β, IL-6, iNOS and VEGF, but not CCL2 and PAI-1. Taken together, these results indicate that CXCR3 signaling inhibits inflammatory response and subsequent neovascularization in the alkali burn model.

3.5. CXCR3 expressed on bone marrow (BM)-derived leukocytes plays a key role in the inhibition of corneal neovascularization after alkali burn

Although CXCR3 is mainly expressed in T lymphocytes, macrophages and natural killer (NK) cells, non-immune cells including fibroblasts, endothelial, epithelial, and smooth muscle cells also express CXCR3 (Clark-Lewis et al., 2003). We intended to specify the contributions of CXCR3 expressed in BM-derived cells vs CXCR3 expressed in corneal cells in alkali burn-induced corneal neovascularization. We generated BM chimeras, in which BM of WT mice was reconstituted with WT BM (WT→WT) or CXCR3$^{-/-}$

BM (CXCR3$^{-/-}$→WT), or BM of CXCR3$^{-/-}$ mice was reconstituted with WT BM (WT→CXCR3$^{-/-}$) (Fig. 6A). At 6 weeks after BM transplantation, alkali burn was applied to these chimeric mice. Corneal neovascularization and corneal opacity in these chimeric mice were imaged at 14 days after alkali burn (Fig. 6B). No differences in corneal opacity were observed among WT→WT, CXCR3$^{-/-}$→WT, WT→CXCR3$^{-/-}$ mice (Fig. 6B and C). However, compared with WT→WT mice (control), corneal neovascularization was increased in CXCR3$^{-/-}$→WT mice (CXCR3 was deleted in leukocytes but intact in corneal cells), but not in WT→CXCR3$^{-/-}$ mice (CXCR3 was deleted in corneal cells but intact in leukocytes) (Fig. 6B and D). Similarly, immunostaining revealed that alkali burn induced larger area of hemangiogenesis in the corneas of CXCR3$^{-/-}$→WT mice than WT→WT and WT→CXCR3$^{-/-}$ mice (Fig. 7A and B) (n = 4, *p < 0.05, **p < 0.01). Nevertheless, there were no differences in lymphangiogenesis among WT→WT, CXCR3$^{-/-}$→WT, WT→CXCR3$^{-/-}$ mice (Fig. 7A and C). These results suggest that CXCR3 expressed in BM-derived leukocytes has a dominant role in inhibiting corneal hemangiogenesis after alkali burn while CXCR3 expressed in both leukocytes and corneal cells is required to inhibit corneal lymphangiogenesis.

4. Discussion

In the course of corneal wound healing, persistent inflammation leads to neovascularization, but the underlying mechanism remains to be determined. Here, we demonstrated that the activation of chemokine receptor CXCR3 is closely involved in corneal neovascularization in a corneal alkali burn model. We found that alkaline burn leads to elevated expression of CXCR3 and its ligand CXCL10 in the cornea. Using transgenic CXCR3$^{-/-}$ mice, we demonstrated that CXCR3 deficiency exaggerated the expression of inflammatory cytokines and VEGF in the cornea, leading to excessive formation of corneal hemangiogenesis and lymphangiogenesis. Finally, BM transplantation model revealed that CXCR3 expressing cells originated from the bone marrow are likely to be the primary cause of corneal neovascularization. This is the first study using a genomics approach to investigate the role of CXCR3 in corneal neovascularization after chemical burn. This study, together with a previous study showing exogenous CXCL10 can effectively reduce the formation of corneal neovascularization and lymphatic vessels in the model of fungal keratitis (Gao et al., 2017), highlighting the potential of the CXCL10/CXCR3 axis as a therapeutic intervention for corneal neovascularization in multiple pathological conditions. Since our goal in the study is to investigate the role of CXCR3 in corneal neovascularization using genetic approaches, we did not perform CXCL10 treatment to assess the therapeutic effects of targeting this pathway. Our follow-up studies will further test the effects of CXCL10 treatment and determine whether its effects are mediated by CXCR3.

Due to corneal angiogenic privilege and immune privilege (Hamrah et al., 2003), only a small amount of inflammatory cells are distributed in normal corneal limbus. After severe corneal injury, inflammatory cells infiltrate into the physiologically non-vascular cornea, and new blood vessels and lymphatic vessels burst from the limbus of the cornea. In general, following corneal injury, the recruitment and activation of inflammatory cells are mediated by pro-inflammatory/angiogenic molecules produced by epithelial cells and other corneal cells at the site of injury. In our study, IL-1β, IL-6, iNOS and VEGF were

sharply upregulated after alkali burn, which were further elevated in CXCR3$^{-/-}$ mice. These factors have proven to be important mediators for leukocytes that can be recruited from the limbal vessels and migrate to the wound site (Hong et al., 2001; Stapleton et al., 2008). At the same time, we used Concanavalin A to label leukocytes and vessels, and found that the number of leukocytes in the vessels of CXCR3$^{-/-}$ cornea was significantly higher than that of WT cornea after alkali burn. These results suggest that CXCR3 deletion exacerbates inflammation and excessive corneal inflammation may lead to a more severe corneal neovascularization and lymphatic vessel formation, which are substantial risk factors for immunological graft rejection (Bachmann et al., 2010; Hos and Cursiefen, 2014).

At present, the exact mechanism of CXCR3 regulating corneal neovascularization remains to be studied. CXCR3 is expressed on newly formed vessels and CXCL10 stimulation inhibits endothelial cell migration and tube formation, promotes dissociation of newly formed blood vessels, and induces endothelial cell death (Bodnar et al., 2009; Yates-Binder et al., 2012). This mechanism accounts for the angiostatic effect of CXCR3 during skin wound repair (Bodnar et al., 2009). However, in our study, through bone marrow transplantation experiment, we found that deleting CXCR3 in bone marrow cells but not in corneal cells significantly enhanced corneal neovascularization, indicating that CXCR3-expressing leukocytes were the main factor contributing to the angiostatic effect of CXCR3 in the cornea after alkali burn. We speculate that a subtype(s) of CXCR3-expressing leukocytes are recruited to the cornea after alkali burn and this subtype(s) of cells may exhibit anti-inflammatory and anti-angiogenic property. Future studies are needed to test this possibility and identify this group of cells to better understand the mechanisms by which CXCR3 inhibits angiogenesis in the cornea. Lymphangiogenesis, however, was not altered by deleting CXCR3 in bone marrow cells or local cells in the cornea, suggesting different mechanisms are involved in hemangiogenesis and lymphangiogenesis. Interestingly, while activation of CXCR3 is beneficial in corneal alkali injury, fungal keratitis and herpes simplex virus 1 infection (Gao et al., 2017; Wuest and Carr, 2008), deletion of CXCR3 attenuates inflammatory response and prevents retinal ganglion cell loss in mouse models of retinal ischemia-reperfusion and optic nerve crush (Ha et al., 2015, 2017). Therefore, activation of CXCR3 may elicit different pathophysiology dependent on the contexts of cells, tissues and diseases. Tissue specific regulation of this pathway, rather than systemic activation or blockade, is more desired when targeting it for disease therapy.

In conclusion, using genomics approach along with advanced imaging tools, the current study explored the influence of chemokine receptor CXCR3 activation in promoting corneal neovascularization in an alkali burn model. Specifically, our findings reveal that the CXCR3 pathway contributes significantly to the inhibition of corneal inflammation and neovascularization during the acute phase of wound repair in an alkali burn model and that CXCR3 deficiency amplifies ocular inflammation, resulting in increased corneal hemangiogenesis and lymphangiogenesis. While the current study highlights the potential of the CXCL10/CXCR3 axis as a therapeutic intervention for corneal neovascularization, it should be noted that since CXCR3 is not the only member of the chemokine receptor family, further study of the therapeutic role of other chemokines and chemokine receptors in acute and chronic corneal inflammation is warranted.

Supplementary Material

Refer to Web version on PubMed Central for supplementary material.

Funding information

This work was supported in part by National Institutes of Health grants EY034266, EY026629 and EY022694, and UT System Faculty STARs Award (to W.Z.); and National Institutes of Health grant EY031054 (to H.L.); and NIEHS T32ES007254 (to J. L.).

Abbreviations:

BM	Bone marrow
OCT	Optical Coherence Tomography
qRT-PCR	Quantitative real-time polymerase chain reaction
VEGF	Vascular endothelial growth factor
WT	Wild type

References

Anderson C, Zhou Q, Wang S, 2014. An alkali-burn injury model of corneal neovascularization in the mouse. JoVE 86, 51159.

Bachmann B, Taylor RS, Cursiefen C, 2010. Corneal neovascularization as a risk factor for graft failure and rejection after keratoplasty: an evidence-based meta-analysis. Ophthalmology 117, 1300–1305 e1307. [PubMed: 20605214]

Bodnar RJ, Yates CC, Rodgers ME, Du X, Wells A, 2009. IP-10 induces dissociation of newly formed blood vessels. J. Cell Sci 122, 2064–2077. [PubMed: 19470579]

Clark-Lewis I, Mattioli I, Gong JH, Loetscher P, 2003. Structure-function relationship between the human chemokine receptor CXCR3 and its ligands. J. Biol. Chem 278, 289–295. [PubMed: 12417585]

de Jong EK, de Haas AH, Brouwer N, van Weering HR, Hensens M, Bechmann I, Pratley P, Wesseling E, Boddeke HW, Biber K, 2008. Expression of CXCL4 in microglia in vitro and in vivo and its possible signaling through CXCR3. J. Neurochem 105, 1726–1736. [PubMed: 18248618]

Donshik PC, Berman MB, Dohlman CH, Gage J, Rose J, 1978. Effect of topical corticosteroids on ulceration in alkali-burned corneas. Arch. Ophthalmol 96, 2117–2120. [PubMed: 214063]

Eslani M, Baradaran-Rafii A, Movahedan A, Djalilian AR, 2014. The ocular surface chemical burns. J Ophthalmol 2014, 196827. [PubMed: 25105018]

Gao N, Liu X, Wu J, Li J, Dong C, Wu X, Xiao X, Yu FX, 2017. CXCL10 suppression of hem- and lymph-angiogenesis in inflamed corneas through MMP13. Angiogenesis 20, 505–518. [PubMed: 28623423]

Giannaccare G, Pellegrini M, Bovone C, Spena R, Senni C, Scorcia V, Busin M, 2020. Anti-VEGF treatment in corneal diseases. Curr. Drug Targets 21, 1159–1180. [PubMed: 32189591]

Ha Y, Liu H, Xu Z, Yokota H, Narayanan SP, Lemtalsi T, Smith SB, Caldwell RW, Caldwell RB, Zhang W, 2015. Endoplasmic reticulum stress-regulated CXCR3 pathway mediates inflammation and neuronal injury in acute glaucoma. Cell Death Dis. 6, e1900. [PubMed: 26448323]

Ha Y, Liu H, Zhu S, Yi P, Liu W, Nathanson J, Kayed R, Loucas B, Sun J, Frishman LJ, Motamedi M, Zhang W, 2017. Critical role of the CXCL10/C-X-C chemokine receptor 3 Axis in promoting leukocyte recruitment and neuronal injury during traumatic optic neuropathy induced by optic nerve crush. Am. J. Pathol 187, 352–365. [PubMed: 27960090]

Hamrah P, Huq SO, Liu Y, Zhang Q, Dana MR, 2003. Corneal immunity is mediated by heterogeneous population of antigen-presenting cells. J. Leukoc. Biol 74, 172–178. [PubMed: 12885933]

Hong JW, Liu JJ, Lee JS, Mohan RR, Mohan RR, Woods DJ, He YG, Wilson SE, 2001. Proinflammatory chemokine induction in keratocytes and inflammatory cell infiltration into the cornea. Invest. Ophthalmol. Vis. Sci 42, 2795–2803. [PubMed: 11687520]

Hos D, Cursiefen C, 2014. Lymphatic vessels in the development of tissue and organ rejection. Adv. Anat. Embryol. Cell Biol 214, 119–141. [PubMed: 24276891]

Keating AM, Jacobs DS, 2011. Anti-VEGF treatment of corneal neovascularization. Ocul. Surf 9, 227–237. [PubMed: 22023817]

Kim DH, Im ST, Yoon JY, Kim S, Kim MK, Chung MH, Park CK, 2021. Comparison of therapeutic effects between topical 8-oxo-2'-deoxyguanosine and corticosteroid in ocular alkali burn model. Sci. Rep 11, 6909. [PubMed: 33767351]

Kim TI, Chung JL, Hong JP, Min K, Seo KY, Kim EK, 2009. Bevacizumab application delays epithelial healing in rabbit cornea. Invest. Ophthalmol. Vis. Sci 50, 4653–4659. [PubMed: 19458331]

Kobayashi A, Shirao Y, Yoshita T, Yagami K, Segawa Y, Kawasaki K, Shozu M, Tseng SC, 2003. Temporary amniotic membrane patching for acute chemical burns. Eye 17, 149–158. [PubMed: 12640400]

Koenig Y, Bock F, Horn F, Kruse F, Straub K, Cursiefen C, 2009. Short- and long-term safety profile and efficacy of topical bevacizumab (Avastin) eye drops against corneal neovascularization. Graefes Arch. Clin. Exp. Ophthalmol 247, 1375–1382. [PubMed: 19415316]

Lange S, Haigis W, Grein HJ, Schutze J, 2009. Comparison of different optical techniques for determination of the dimensions of anterior ocular segment. Klin Monbl Augenheilkd 226, 485–490. [PubMed: 19449280]

Leibowitz HM, 1980. Management of inflammation in the cornea and conjunctiva. Ophthalmology 87, 753–758. [PubMed: 7443202]

Li S, Shi S, Luo B, Xia F, Ha Y, Merkley KH, Motamedi M, Zhang W, Liu H, 2022. Tauopathy induces degeneration and impairs regeneration of sensory nerves in the cornea. Exp. Eye Res 215, 108900. [PubMed: 34929160]

Li Y, Shi S, Xia F, Shan C, Ha Y, Zou J, Adam A, Zhang M, Wang T, Liu H, Shi PY, Zhang W, 2021. Zika virus induces neuronal and vascular degeneration in developing mouse retina. Acta Neuropathol Commun 9, 97. [PubMed: 34034828]

Liu W, Ha Y, Xia F, Zhu S, Li Y, Shi S, Mei FC, Merkley K, Vizzeri G, Motamedi M, Cheng X, Liu H, Zhang W, 2020. Neuronal Epac1 mediates retinal neurodegeneration in mouse models of ocular hypertension. J. Exp. Med 217.

Luisi J, Kraft ER, Giannos SA, Patel K, Schmitz-Brown ME, Reffatto V, Merkley KH, Gupta PK, 2021. Longitudinal assessment of alkali injury on mouse cornea using anterior segment optical coherence Tomography. Transl Vis Sci Technol 10, 6.

Nicholas MP, Mysore N, 2021. Corneal neovascularization. Exp. Eye Res 202, 108363. [PubMed: 33221371]

Philipp W, Speicher L, Humpel C, 2000. Expression of vascular endothelial growth factor and its receptors in inflamed and vascularized human corneas. Invest. Ophthalmol. Vis. Sci 41, 2514–2522. [PubMed: 10937562]

Rappert A, Bechmann I, Pivneva T, Mahlo J, Biber K, Nolte C, Kovac AD, Gerard C, Boddeke HW, Nitsch R, Kettenmann H, 2004. CXCR3-dependent microglial recruitment is essential for dendrite loss after brain lesion. J. Neurosci 24, 8500–8509. [PubMed: 15456824]

Sharif Z, Sharif W, 2019. Corneal neovascularization: updates on pathophysiology, investigations & management. Rom J Ophthalmol 63, 15–22. [PubMed: 31198893]

Spiteri N, Romano V, Zheng Y, Yadav S, Dwivedi R, Chen J, Ahmad S, Willoughby CE, Kaye SB, 2015. Corneal angiography for guiding and evaluating fine-needle diathermy treatment of corneal neovascularization. Ophthalmology 122, 1079–1084. [PubMed: 25841974]

Stapleton WM, Chaurasia SS, Medeiros FW, Mohan RR, Sinha S, Wilson SE, 2008. Topical interleukin-1 receptor antagonist inhibits inflammatory cell infiltration into the cornea. Exp. Eye Res 86, 753–757. [PubMed: 18346730]

Tarff A, Drew-Bear LE, Di Meglio L, Yee R, Vizcaino MA, Gupta P, Annadanam A, Cano M, Behrens A, 2022. Effect of topical bovine colostrum in wound healing of corneal surface after acute ocular alkali burn in mice. Exp. Eye Res 220, 109093. [PubMed: 35490838]

Torraca V, Cui C, Boland R, Bebelman JP, van der Sar AM, Smit MJ, Siderius M, Spaink HP, Meijer AH, 2015. The CXCR3-CXCL11 signaling axis mediates macrophage recruitment and dissemination of mycobacterial infection. Dis Model Mech 8, 253–269. [PubMed: 25573892]

Vivanco-Rojas O, Garcia-Bermudez MY, Iturriaga-Goyon E, Rebollo W, Buentello-Volante B, Magana-Guerrero FS, Bates P, Perez-Torres A, Garfias Y, 2020. Corneal neovascularization is inhibited with nucleolin-binding aptamer, AS1411. Exp. Eye Res 193, 107977. [PubMed: 32081668]

Wang HY, Wei RH, Zhao SZ, 2012. [Research status of photodynamic therapy for corneal neovascularization]. Zhonghua Yan Ke Za Zhi 48, 662–665. [PubMed: 22943874]

Wuest TR, Carr DJ, 2008. Dysregulation of CXCR3 signaling due to CXCL10 deficiency impairs the antiviral response to herpes simplex virus 1 infection. J. Immunol 181, 7985–7993. [PubMed: 19017990]

Xia F, Ha Y, Shi S, Li Y, Li S, Luisi J, Kayed R, Motamedi M, Liu H, Zhang W, 2021. Early alterations of neurovascular unit in the retina in mouse models of tauopathy. Acta Neuropathol Commun 9, 51. [PubMed: 33762004]

Yates-Binder CC, Rodgers M, Jaynes J, Wells A, Bodnar RJ, Turner T, 2012. An IP-10 (CXCL10)-derived peptide inhibits angiogenesis. PLoS One 7, e40812. [PubMed: 22815829]

Yates CC, Whaley D, Hooda S, Hebda PA, Bodnar RJ, Wells A, 2009. Delayed reepithelialization and basement membrane regeneration after wounding in mice lacking CXCR3. Wound Repair Regen. 17, 34–41 [PubMed: 19152649]

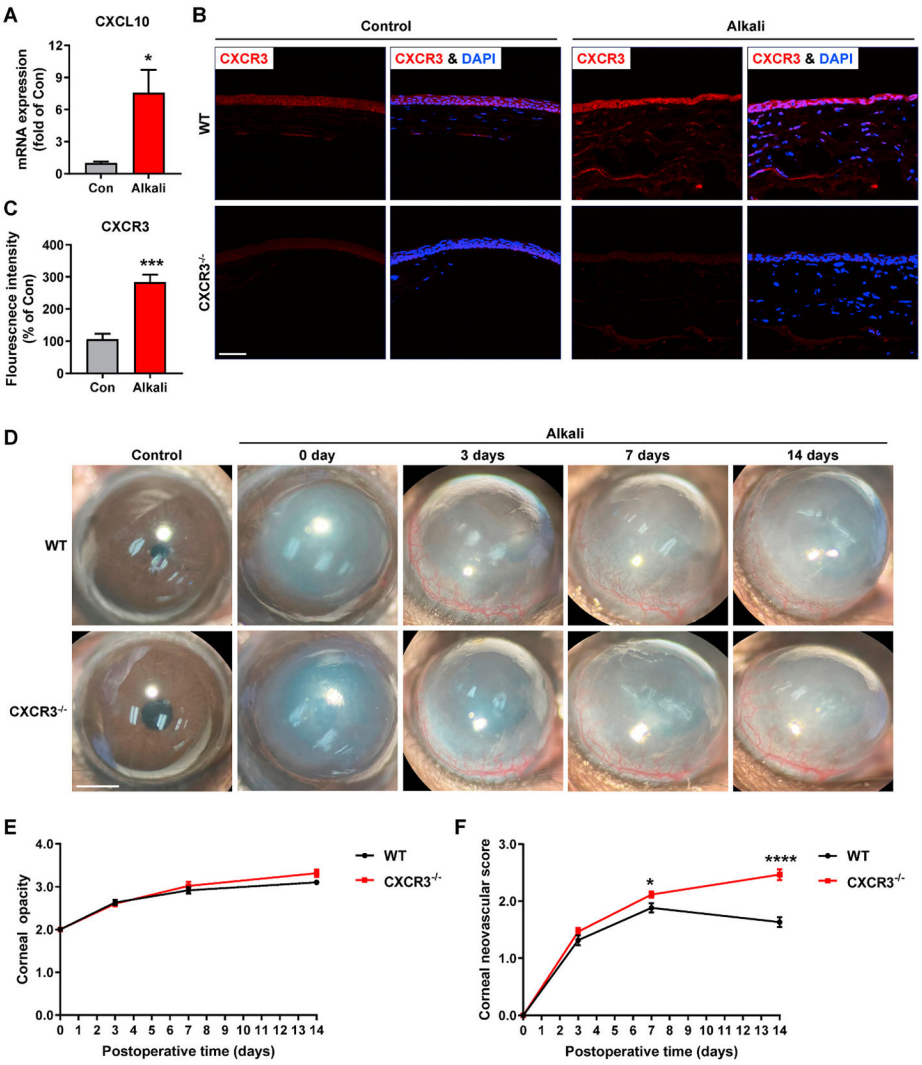

Fig. 1. CXCR3 signaling is involved in alkali burn-induced corneal neovascularization.

(A–C) Corneas or eyeballs were collected from WT and CXCR3$^{-/-}$ mice at 3 days after alkali burn. CXCL10 expression in the cornea was measured by RT-PCR (A). Corneal sections were stained with anti-CXCR3 antibody (red) and the fluorescence intensity of CXCR3 was quantified (B, C). Scale bar: 50 μm. n = 4–5; *p < 0.05 and ***p < 0.001. (D–F) The bright field images were taken before alkali burn and at different time points after alkali burn (0, 3, 7 and 14 days). Corneal opacity and neovessel formation were assessed. Scale bar: 1 mm. n = 6; *p < 0.05, and ****p < 0.0001.

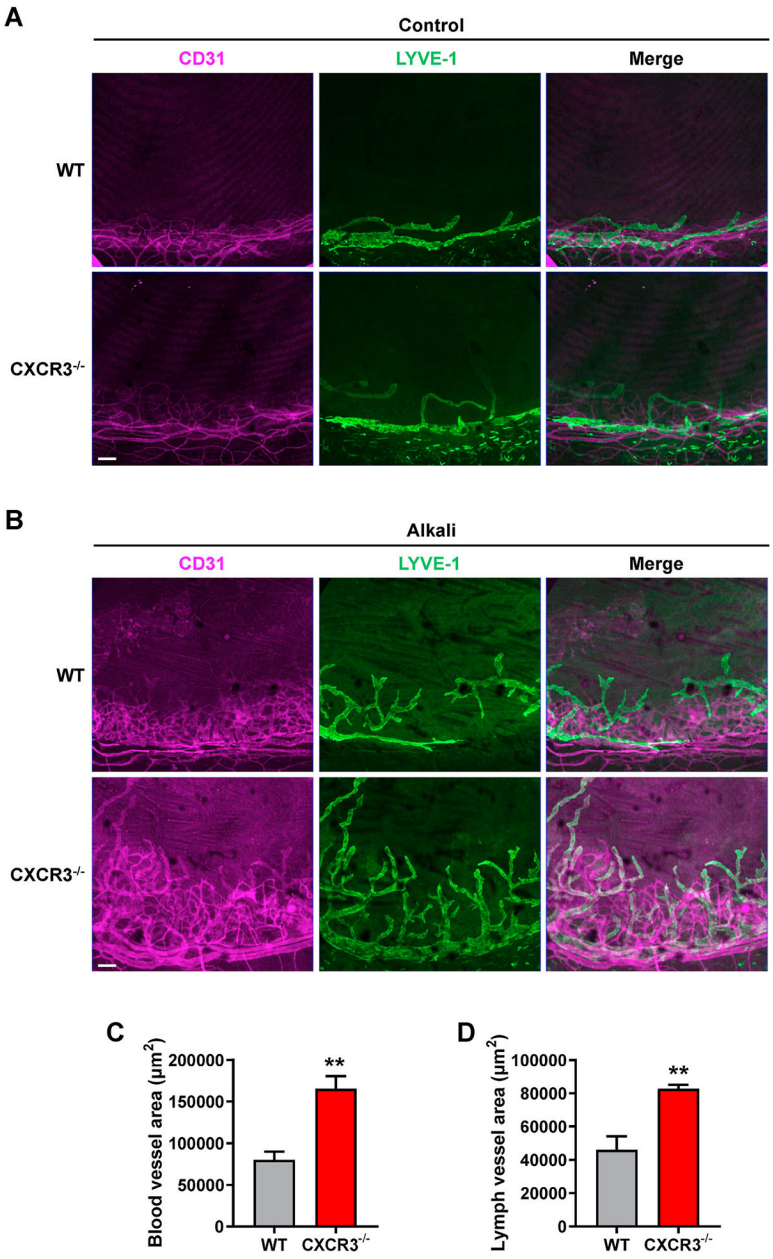

Fig. 2. CXCR3 deficiency aggravates corneal neovascularization in an alkali burn model.

Eyeballs were collected from WT and CXCR3$^{-/-}$ mice at 14 days after alkali burn or control mice. Corneas were stained with anti-CD31 (purple) for blood vessels and anti-LYVE-1 (green) for lymphatic vessels. (A, B) Representative images from control cornea or alkali burned-cornea. (C, D) Quantification of the area of CD31^{+} blood vessels and LYVE-1^{+} lymphatic vessels. Scar bar: 100 μm. n = 5; **p < 0.01.

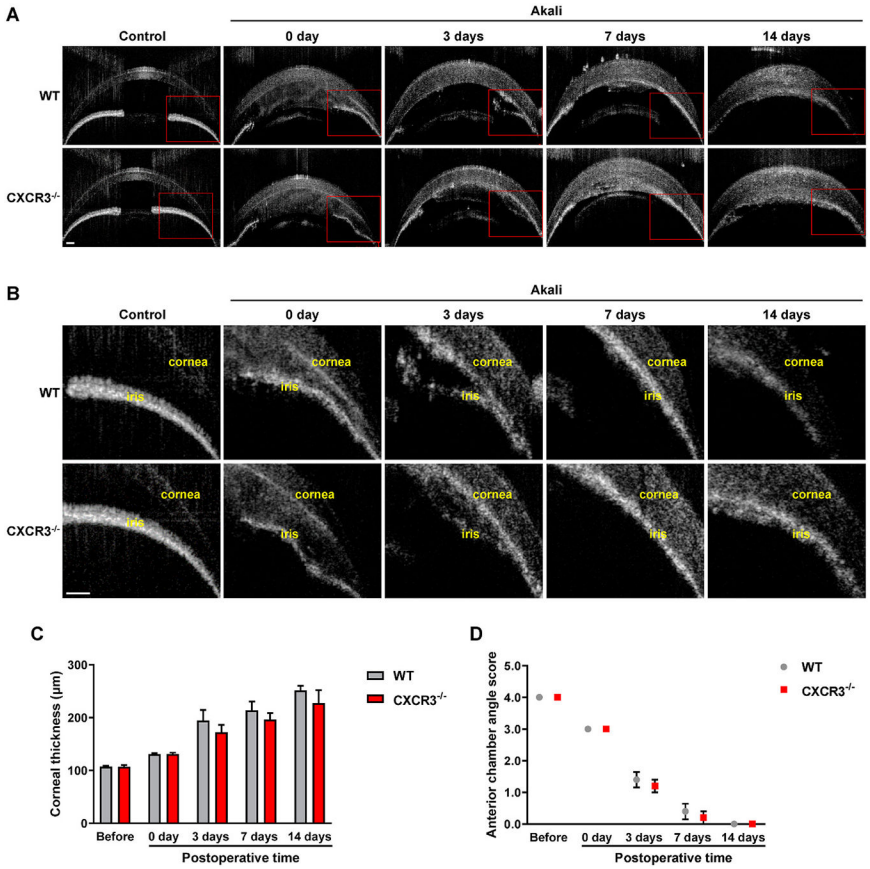

Fig. 3. CXCR3 deficiency does not affect corneal thickness and the closure of anterior chamber angle after alkali burn.

(A, B) Representative images of the anterior segment by OCT at various time points after alkali burn. Anterior chamber angle (red rectangle in A) was zoomed in for the details of angle structure (B). (C) Quantification of the full thicknesses of the cornea. (D) Assessment of anterior chamber angle using the Shaffer grading system. Scar bar: 100 μm. n = 5.

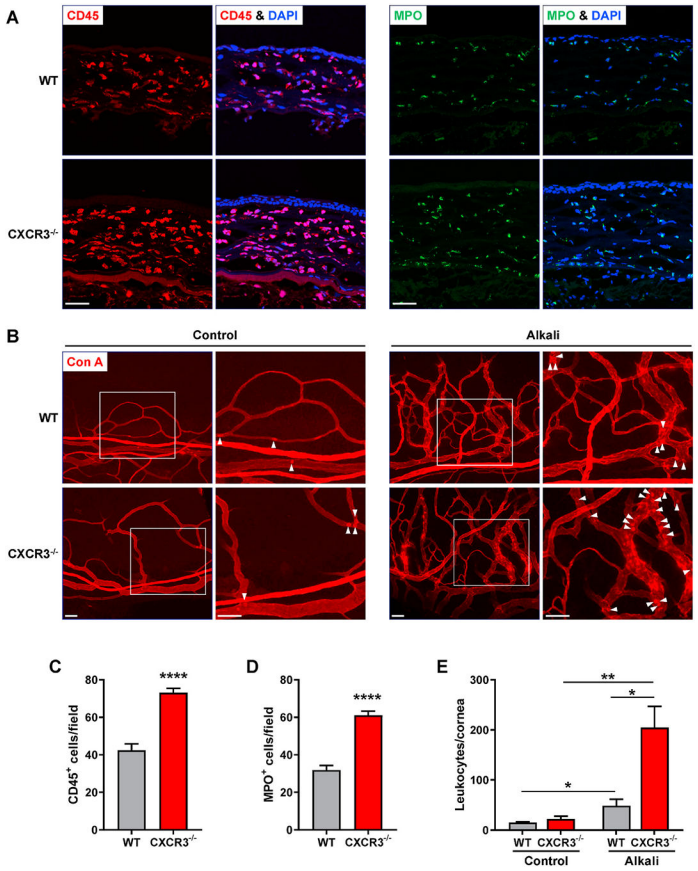

Fig. 4. CXCR3 deficiency aggravates corneal immune cell infiltration and leukostasis after alkali burn.

(A) Eyeballs were collected from WT and CXCR3$^{-/-}$ mice at 3 days after alkali burn and corneas were stained with anti-CD45 (red) and anti-MPO (green). (B) Representative images of leukostasis at 14 days after alkali burn. Leukocytes in vessels were identified as red round cells (white arrowheads). (C–E) Bar graphs represent the number of CD45^{+}, MPO^{+} cells/field and adherent leukocytes/cornea. Scar bar: 50 μm. n = 4–5; *p < 0.05, **p < 0.01, and ****p < 0.0001.

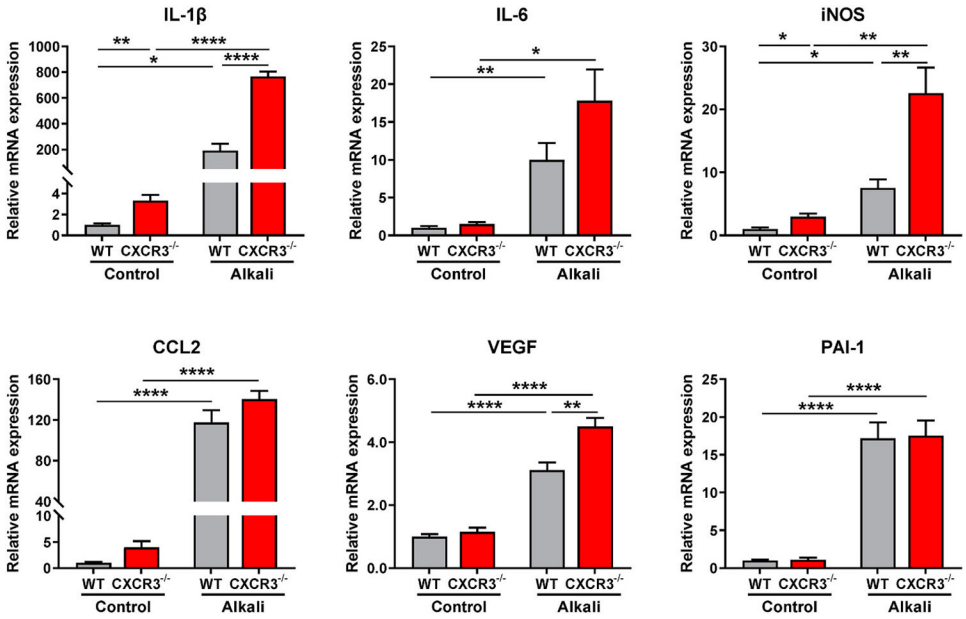

Fig. 5. CXCR3 deletion exaggerates the upregulation of inflammatory and proangiogenic gene expression after alkali burn.

Corneas were collected from WT and CXCR3$^{-/-}$ mice at 3 days after alkali burn. The expression of IL-1β, IL-6, iNOS, CCL2, VEGF and PAI-1 genes in the cornea was measured by RT-PCR. n = 4–5; *p < 0.05, **p < 0.01, and ****p < 0.0001.

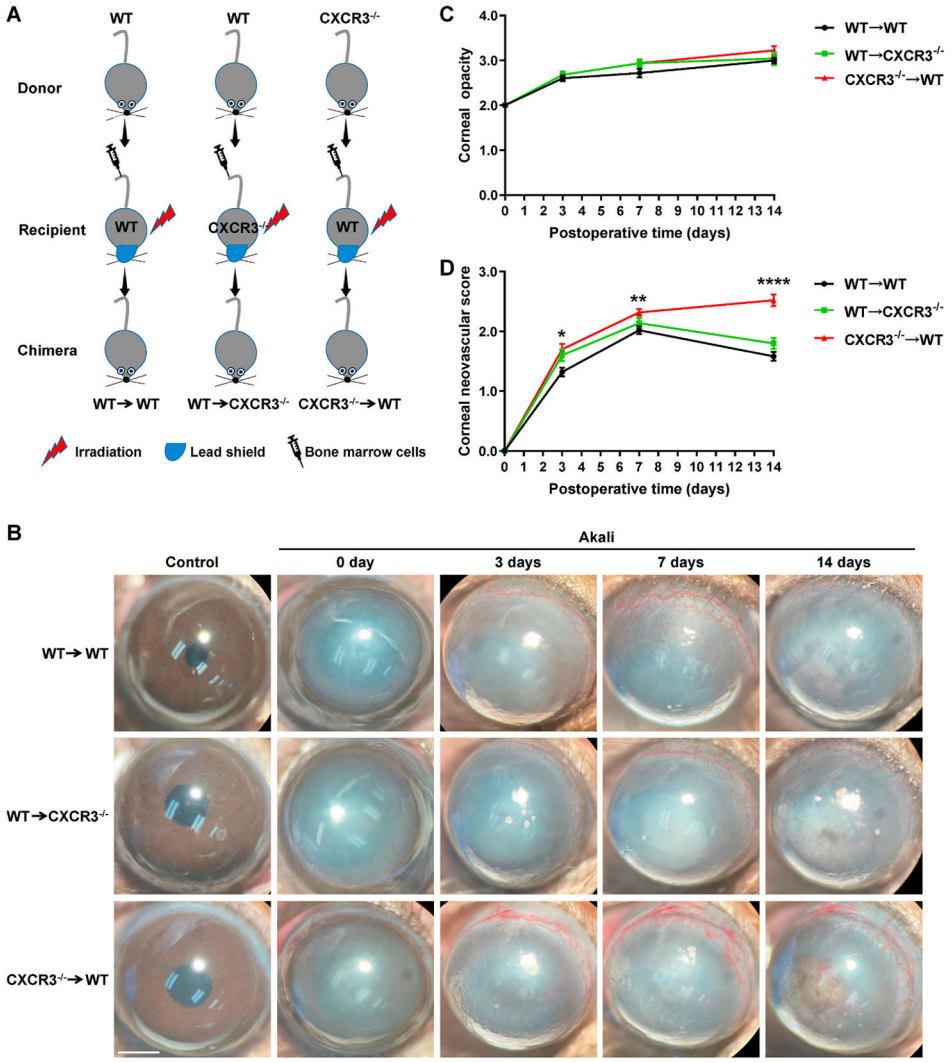

Fig. 6. CXCR3 expression on BM-derived leukocytes is responsible for corneal neovascularization after alkali burn.

(A) Schematic illustration presents different BM transplantation in WT (WT→T and CXCR3$^{-/-}$→WT) and CXCR3$^{-/-}$ (WT→ CXCR3$^{-/-}$) recipients. (B) Representative corneal images were taken before and at various time points after alkali burn (days 0, 3, 7, and 14). (C, D) Clinical assessment of corneal opacity and neovascularization after alkali burn. Scale bar: 1 mm. n = 5; *p < 0.05, **p < 0.01 and ****p < 0.0001 compared with WT→WT.

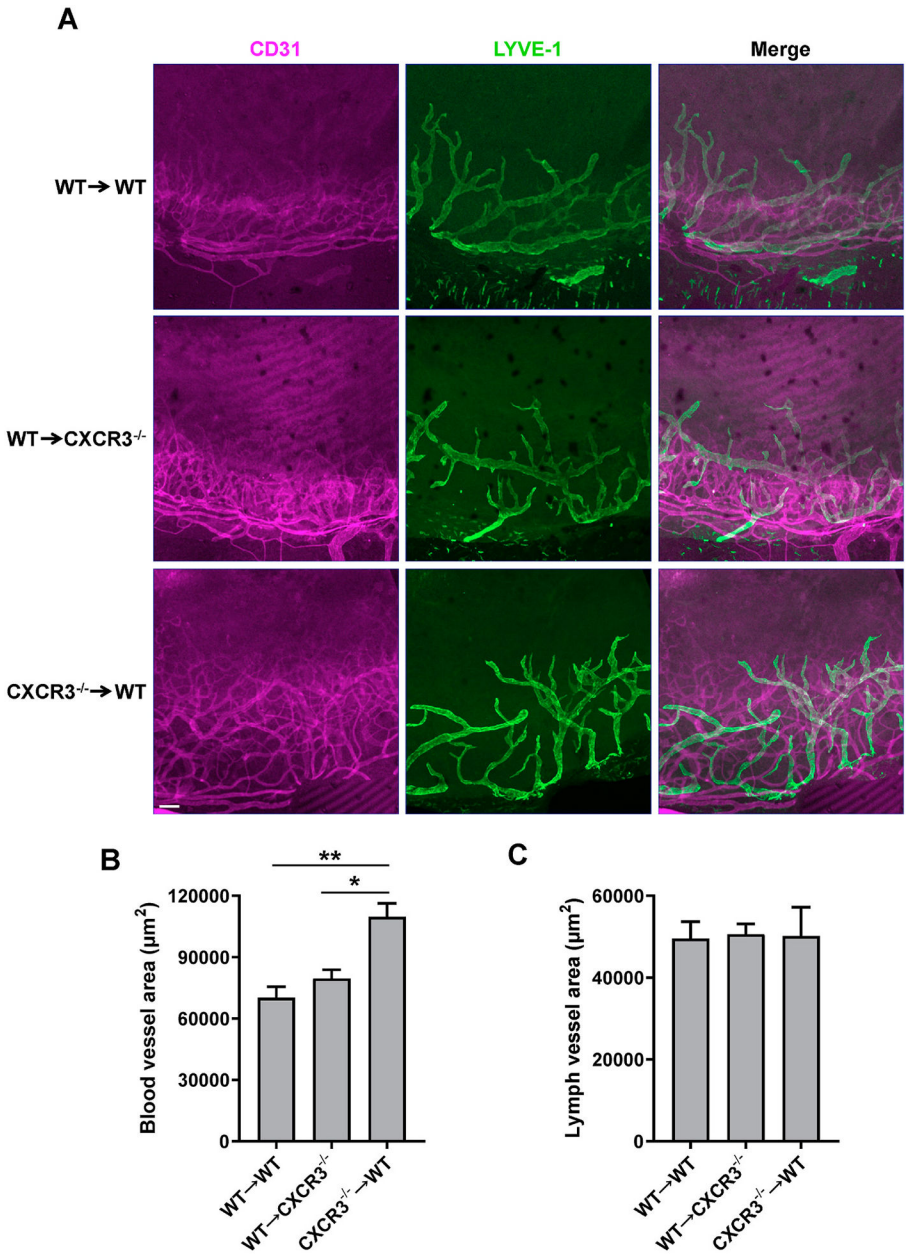

Fig. 7. CXCR3 expression on BM-derived leukocytes is responsible for corneal hemangiogenesis but not lymphangiogenesis after alkali burn.

(A) Representative images of corneal flatmount stained with CD31 antibody (purple) for blood vessels and LYVE-1 antibody (green) for lymphatic vessels. (B, C) Quantification of the area of $CD31^+$ blood vessels and $LYVE\text{-}1^+$ lymphatic vessels. Scar bar: 100 μm. n = 4; *p < 0.05, and **p < 0.01.

Table 1

Primer sequences for RT-PCR.

Gene	Forward	Reverse
CXCL10	GGA CGG TCC GCT GCA A	CCC TAT GGC CCT CAT TCT CA
IL-1β	AGT TGA CGG ACC CCA AAA GA	GGA CAG CCC AGG TCA AAG G
IL-6	CCA CGG CCT TCC CTA CTT C	TTG GGA GTG GTA TCC TCT GTG A
iNOS	GCA GCC TGT GAG ACC TTT G	TGC ATT GGA AGT GAA GCG TTT
CCL2	GGC TCA GCC AGA TGC AGT TAA	CCT ACT CAT TGG GAT CAT CTT GCT
VEGF	TAC CTC CAC CAT GCCAAG TG	TCA TGG GAC TTC TGC TCT CCT T
PAI-1	CGA CAC CCT CAG CAT GTT CA	CGG AGA GGT GCA CAT CTT TCT